

# Open-Phase Fault-Tolerant Direct Torque Control For Five-Phase Five-Level NPC VSI fed Induction Motor Drive

Jampana Vijay Kumar Raju, B. Venkataramana

**Abstract**— The important aspect of multiphase machine (MM) drives is the inherent fault-tolerant capability; thus, suitable for most reliable industrial and transportation applications. A faster dynamic response of the electric motor drive can be achieved by using direct torque control (DTC) technique. In this paper, an open-phase fault (OPF) control scheme enabling DTC is proposed for a Five Phase Five-level induction motor drive. The main scope of the proposed Control technique is needed for interrupt free operation of the FPIM drive even after an OPF occurs. The developed post-fault controller is same for both healthy and post-fault operation. However; the lookup table developed for both healthy and post-fault operations are different. This is due to the OPF condition has different voltage vectors than the healthy condition. The proposed five level converter is verified by Matlab/Simulink results at steady and transient loading operations.

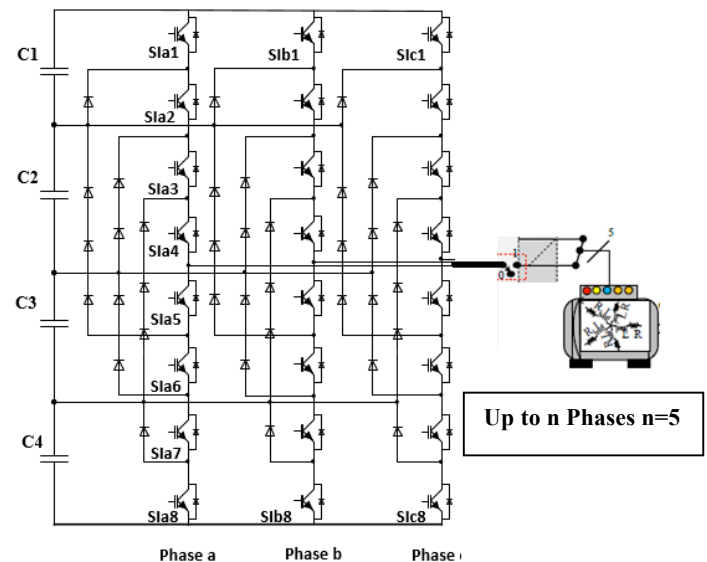
**Index Terms**— Terms—fault-tolerant torque control, induction motor drive, phase fault detection, three-level NPC VSI.

## I. INTRODUCTION

The reliability of high power variable speed drives [1] is a new upcoming challenges especially in applications like high-powered electric and hybrid electric vehicles, off-shore ship propulsion, more-electric aircraft, etc. [2]–[5]. For this, the multiphase machines (MM) are best alternative option instead of three-phase machines [6]–[10] due to two significant concerns. Firstly, the interrupt free operation of MM drives is possible with increased phase numbers i.e, the  $n$  (odd) phase machine can run with up to  $n-1$  number of phases faulty [3]. Second, with the increase in phase number, per phase requirement of drive power control capability reduces; thus, the use of series/parallel configuration of power switches can be minimized. Due to the inherent fault-tolerant operation, the MM drives provide reliable operations without any extra hardware as compared to counter part.

The five-phase induction motor (FPIM) drive has promising outcomes over other MM drives, hence in this paper the FPIM drive is considered to implement the proposed direct torque controller (DTC). Various control techniques like rotor field oriented control (RFOC) and vector control

techniques are equally valid for the MM drives with necessary modifications.



In vector control, the DTC is more advantageous than the other control techniques due to its advantages such as less parameters dependency, high dynamic performance [11]. Various DTC techniques are presented for the two-level voltage source inverter (VSI) fed MM drives in [12]. For medium and highpower drives, the three-level NPC is most accepted VSI in industry due to improved THD and low  $dv=dt$ , common mode voltage (CMV) as compared to two-level VSI [4], [12]. Also, as level of inverter increases the possible available voltage vectors are high and hence, the combination of vectors are more to develop the good closed loop control. Under the normal operation, various DTC schemes for three-level NPC VSI fed FPIM drive is presented in [12].

The fault-tolerant operation consists of three major objectives, a) fault detection, b) fault localisation and c) post-fault control strategy. Out of which, (a) and (b) are not in the scope of this paper. However, the proposed method uses the fault detection method based on the vector space decomposed method [13], [14]. In healthy operation, control techniques of the FPIM drive are equally valid for the post-fault situation. But, the control structure need to be modified under an open phase fault (OPF) condition due to loss of phases [14], [15]. In [14], an open-phase fault (OPF) enabled DTC is introduced for the two-level (2L) VSI fed FPIM drive with virtual vector (VV) concept. A quantitative analysis is performed between RFOC, model predictive control (MPC) and DTC in [15]. The MPC scheme is good

**Jampana Vijay Kumar Raju**, Electrical and electronics Engineering, Avanthi's st theressa institute of engineering and technology, Vizinagaram, India.

**B. Venkataramana**, Electrical and electronics Engineering, Avanthi's st theressa institute of Engineering and technology, Vizinagaram, India.

competitor for the DTC method. However, this method has more complexity in implementation, as inverter level increase. Also, the cost function need to be changed under the post-fault condition.

Nevertheless, an interrupt-free post-fault investigation can only be accomplished while the closed-loop control of FPIM drive is capable of self-configurable control action. For this, the reconfigure-less control scheme has been developed for the 2L-VSI fed FPIM [14]. The mentioned method is therefore restricted to an FPIM drive fed with 2L-VSI. The post fault control strategies provided in [13] are limited to five level NPC VSI fed FPIM drive operation.

Therefore, in this paper, the post-fault DTC scheme is developed to continue the drive operation after an OPF appears in the drive. The proposed study has a major advantage is that the controller reconfiguration is not required, when fault appears in the system. However, the pre-stored lookup tables are different for both pre and post-fault activity.

II. FPIM DRIVE WITH PROPOSED FIVE-LEVEL NPC IN NORMAL AND POST-FAULT CONDITION

The five-level NPC VSI is shown in Fig. 1 with switch port (marked in red; Normal: switch is ON, Faulty: switch is OFF) indication for the OPF insist in one phase of the drive. Where, the power converter switches indicated Sa1 and Sa3 are complementary to each other, similarly Sa2 and Sa4 are complementary with one another. The available states for each Five-level NPC leg are 1, 1/2, 0, -1/2, and -1 and hence, the possible switching voltage vectors are  $35 = 243$  under normal operating conditions [12]. For post-fault activity with an OPF condition, the possible voltage vector combinations are restricted to 81 ( $34 = 81$ ), which are derived using (1) and (2). Out of 81 vectors, 20 vectors are preferred for the proposed DTC scheme using the phase voltage relation and proper sector segments and are projected in  $\alpha$ -frame and xy-frame as presented in Fig. 2.2 and Fig. 2.3, respectively.

The available VVs are mapped in  $\alpha$  and xy plane by considering the post-fault conversion matrix (tx) and stator phase voltages (1) [14]. From these voltage vectors, the post-fault DTC method is developed to obtain the reconfigure-less interrupt free drive operation under the OPF condition

The stator winding of FPIM is fed from the five phase supply, a revolving field will be developed due to the currents produced in the stator. The total flux is analyzed at various instants in terms of maximum flux at different instants. Here,  $\phi_a, \phi_b, \phi_c, \phi_d, \phi_e$ , is flux produced by the respective phases a, b, c, d, e etc., and shown in Figure 1 with a phase delay of 720 as the developed stator currents are also in phase delay of 720. In the conventional supply, the total flux produced by three phases is 1.5 times of the maximum flux. But this should be varied in the case of the proposed motor, analyzed by the produced flux in all the five phases at several instants which are shown below in five modes.

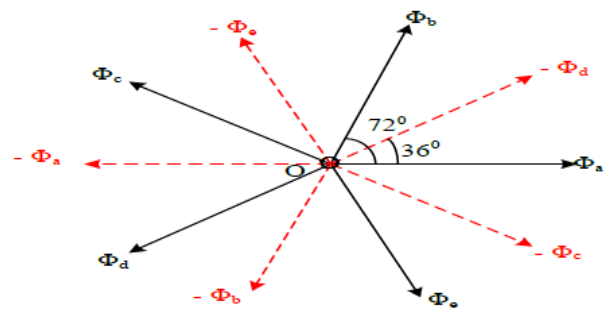


Figure 2.1 Flux Produced in Five Phases by FPIM

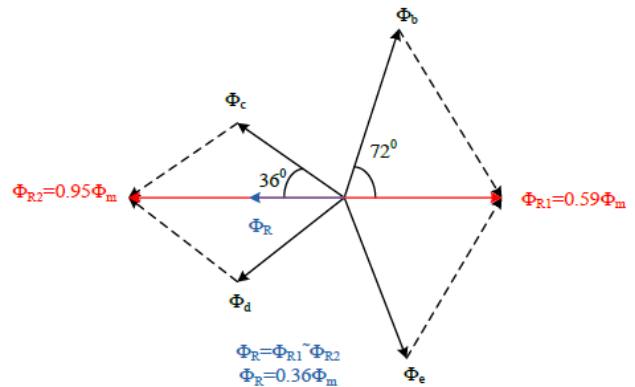


Figure 2.2 Resultant Flux Analyzed in Mode 1

The revolving flux rotates at constant speed around the air gap of the proposed FPIM. In this mode I, the resultant flux is analyzed in terms of maximum flux from phasor diagram shown in Figure 2.

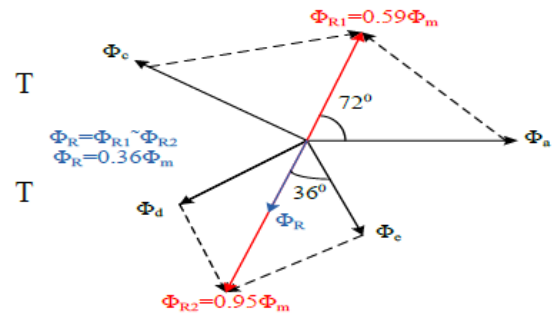


Figure 2.3 Resultant Flux Analyzed in Mode 2

In this mode 2, the resultant flux is analyzed in terms of maximum flux from phasor diagram shown in Figure 3. At  $\omega t = 72^\circ$ .

$$\begin{aligned} \phi_a &= 0.95, \quad \phi_b = 0, \quad \phi_c = 0.95\phi_m \\ \phi_d &= 0.59\phi_m, \quad \phi_e = 0.95\phi_m \end{aligned}$$

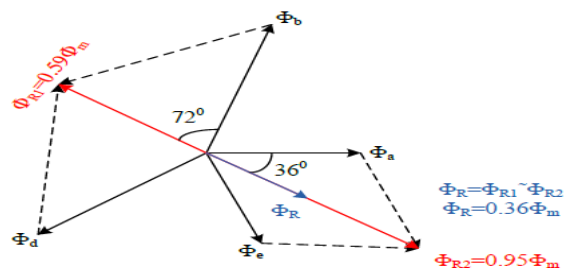


Figure 2.4 Resultant Flux Analyzed in Mode 3

In this mode 3, the resultant flux is analyzed in terms of maximum flux from phasor diagram shown in Figure 4. At  $\omega t = 144^\circ$

$$\varphi_a = 0.59\varphi_m, \varphi_b = 0.95\varphi_m, \varphi_c = 0$$

$$\varphi_d = 0.95\varphi_m, \varphi_e = 0.59\varphi_m$$

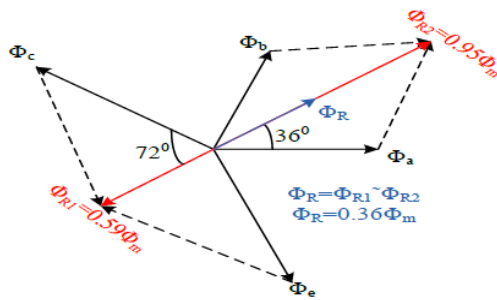


Figure 2.5 Resultant Flux Analyzed in Mode 4

In this mode 4, the resultant flux is analyzed in terms of maximum flux from phasor diagram shown in Figure 5. At  $\omega t=216^\circ$

$$\varphi_a = 0.59\varphi_m, \varphi_b = 0.59\varphi_m, \varphi_c = 0.95\varphi_m$$

$$\varphi_d = 0, \varphi_e = 0.95\varphi_m$$

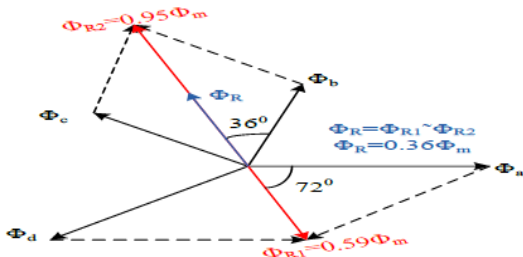


Figure 2.6 Resultant Flux Analyzed in Mode 5

In this mode 5, the resultant fluxes are analyzed in terms of maximum flux from phasor diagram shown in Figure 6. At  $\omega t=288^\circ$

$$\varphi_a = 0.95\varphi_m, \varphi_b = 0.59\varphi_m, \varphi_c = 0.59\varphi_m$$

$$\varphi_d = 0.95\varphi_m, \varphi_e = 0$$

### III. MATHEMATIC LE MODAL FOR FIVE PHASE INDUCTION MOTOR

The state variables are presumed to be the structure of the supply voltages. Representing the supply voltages as

$$v_{bs} = \text{Re}(v_{bss} e^{j\theta_e})$$

$$v_{bss} = V_m e^{-j\alpha}$$

$$v_{cs} = \text{Re}(v_{css} e^{j\theta_e})$$

$$v_{css} = V_m e^{-j2\alpha}$$

$$v_{ds}^a = \text{Re}(v_{dss}^a e^{j\theta_e})$$

$$v_{dss}^a = V_m e^{j2\alpha}$$

$$v_{es} = \text{Re}(v_{ess} e^{j\theta_e})$$

$$v_{bss} = V_m e^{-j\alpha}$$

where  $V_m$  represents peak value of the phase voltage. In view of the form of the supply phase voltages, the state variables and the input voltages are therefore defined. In attaining the model equations based on the harmonic balance technique,

The transformation matrix of arbitrary reference frame is given by

$$T(x) = \frac{2}{5} \begin{bmatrix} \cos(x) & \cos(x-\alpha) & \cos(x-2\alpha) & \cos(x+2\alpha) & \cos(x+\alpha) \\ \sin(x) & \sin(x-\alpha) & \sin(x-2\alpha) & \sin(x+2\alpha) & \sin(x+\alpha) \\ \cos(x) & \cos(x-2\alpha) & \cos(x+\alpha) & \cos(x-\alpha) & \cos(x+2\alpha) \\ \sin(x) & \sin(x-2\alpha) & \sin(x+\alpha) & \sin(x-\alpha) & \sin(x+2\alpha) \\ \frac{1}{2} & \frac{1}{2} & \frac{1}{2} & \frac{1}{2} & \frac{1}{2} \end{bmatrix}$$

where  $\theta$  is the transformation angle of arbitrary reference frame.  $\theta$  is for the stator stationary reference variable transformation and  $\theta$  is for the corresponding rotor variable transformation, where  $\theta$  is the electrical rotor angle.

Therefore, the variables of machine can be transformed to  $q d, x, y, z$  variables as is the variable matrix consisting of voltages, fluxes and currents in reference frame and is the variable matrix consisting of voltages, fluxes and currents in frame of natural reference can respectively be replaced with  $q d, x, y, z$  and for stator and rotor variables respectively

The electromagnetic torque  $T_e$  is given by

$$T_e = \frac{mP}{4} \frac{L_m}{L_r} (\lambda_{dr}' i_{qs} - \lambda_{qr}' i_{ds})$$

$$\frac{2J}{P} p \omega_r = T_e - T_L$$

Where  $m$  is the number of phases,  $P$  is the number of poles,  $J$  represents moment of inertia, and  $T_L$  represents load torque.

### MODELING OF FPMD FOR OPEN PHASE FAULT

Consider the configuration of Figure 3.1 with a switch connected in series with phase 'a' of the stator winding. Open phase fault occurs when the switch is open such that the supply voltage is disconnected from the machine's phase 'a'.

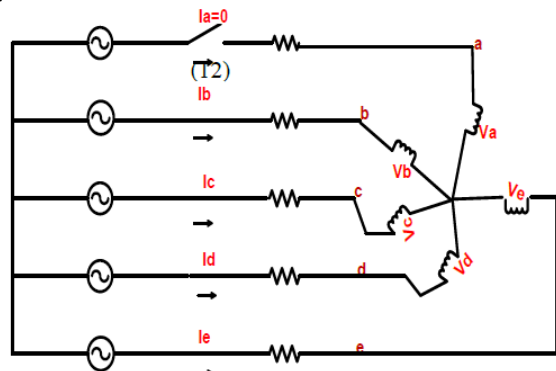


Figure 3.1 Open stator phase Fault 'a' for the FPIM

### IV. MATLAB IMPLEMENTATION AND RESULTS

The validity of the models presented in section 4.1 - 4.2 has been investigated through the computer simulation of the full-order model of the machine with stator phases 'a' and 'b' open-circuited. The steady-state model is used to

calculate the state variables and then the results are compared

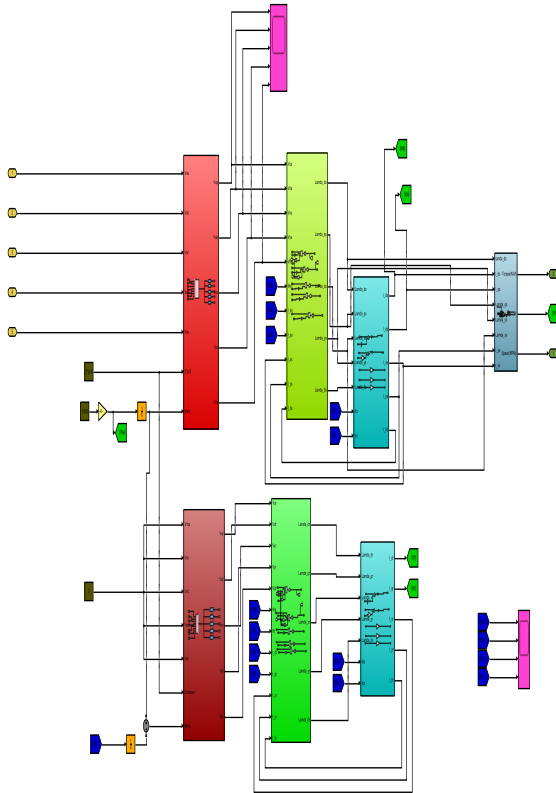


Fig 4.1 Five Phase Induction Motor modal

Five Phase Induction Motor

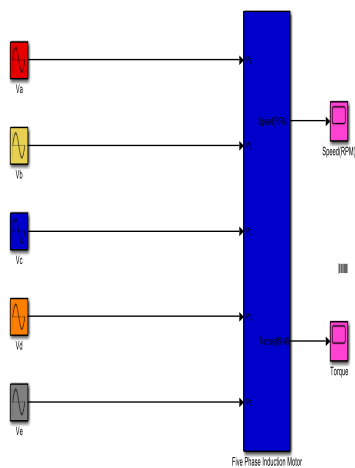


Fig 4.2 Five Phase Induction Motor Subsystem modal

Fig 4.3 has been Represented for Five phase five level NPC multilevel inverter implemented through the computer simulation using matlab Simulink . and Level Shifted PWM Technic Employed to Generated five level out put which is shown fig 4.4.

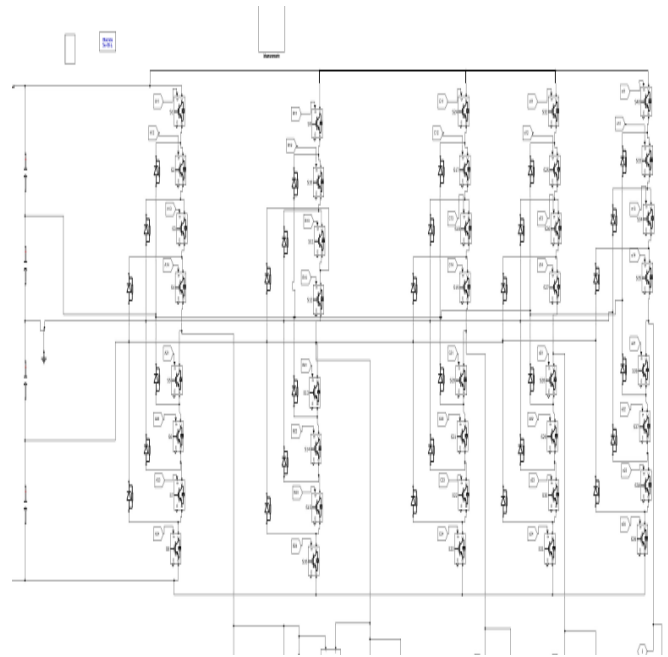


Fig 4.3 Five phase Five Level Diode clamped Inverter

Observe the Figure 10 and 11 the rotor speed and starting torque of the FPIM are 2985 rpm, 32N-m respectively. The experimental values are also tabulated. The settling time of the torque will be 0.6Sec and the magnitude of torque 13.8 N-m. Both simulated and experimental results of speed and torque are approximately equal as shown.



Fig 4.4 Level Shifted Sign PWM Generation

Observe the Fig.4.5 the five phase five level inverter output voltage with 400v, this wave connected five phase induction motor modal( FPIM). Clearly Observe the Figure 4.6 to 4.8 output voltage , motor speed and Motor torque without increasing the voltage under phase loss condition; when one phase loss condition i.e. stator current  $I_e = 0$ , now the magnitude of input and output currents are 3.6A and 2.6A during a period of three cycles with FPIMD.

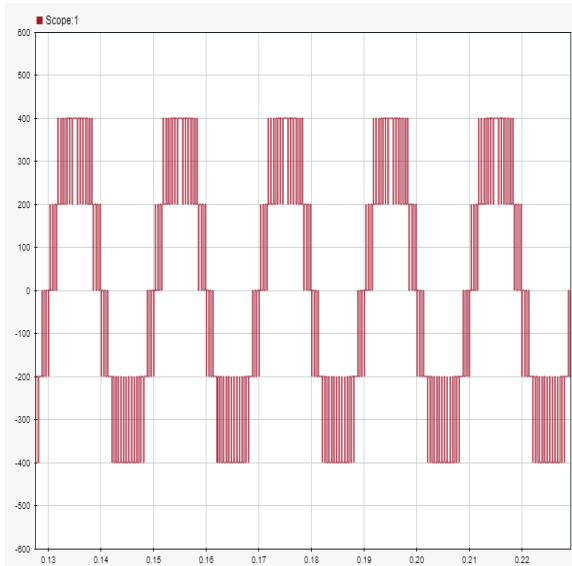


Fig 4.5 Fig Five Lefel Line Voltage

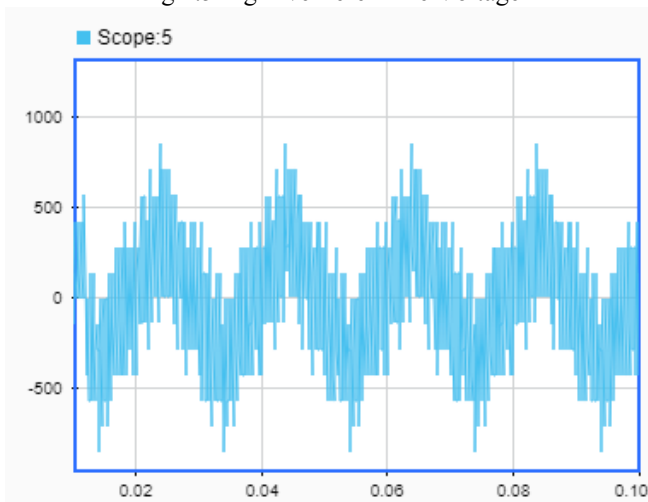


Fig 4.6 Motor Termenal Volage

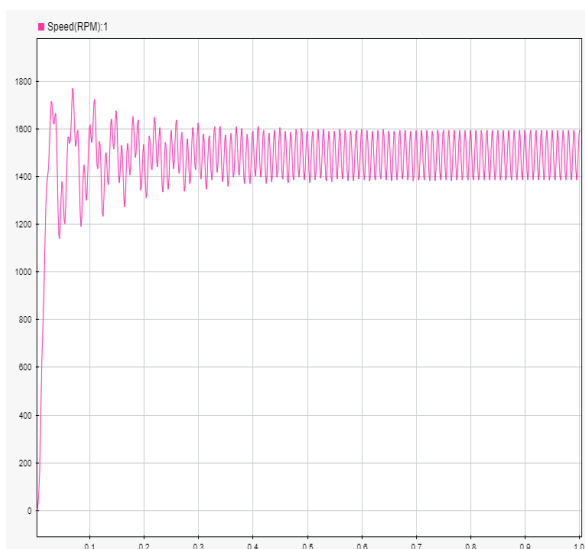


Fig 4.7 Motor Speed

Under phase loss condition; the performance of FPIM does not degrade much. The stator currents are increased when phase loss condition, therefore the advantages of the proposed drive, without increasing the voltage, the stator currents are increased with minimum torque ripple in the drive. Hence the reliability of the drive, gets enhanced.

During the phase loss environment of FPIM, there is no change in the input and output voltages. But if the speed and torque are changed slightly, the results are shown both simulated using MATLAB/SIMULINK

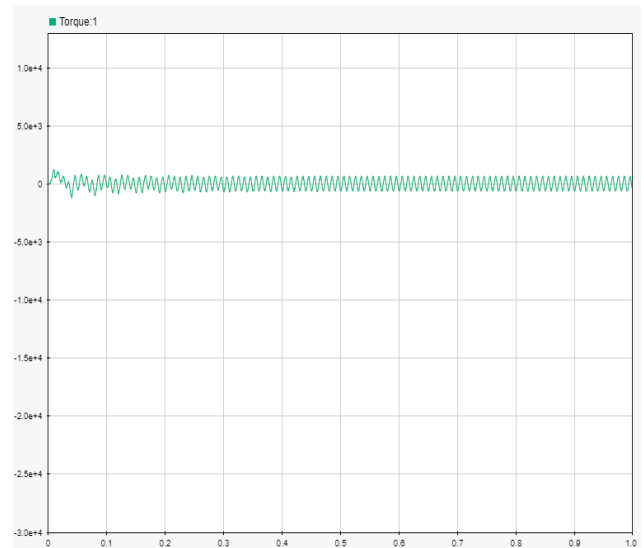


Fig 4.8 Motor Torque

## V. CONCLUSION

The proposed post-fault Control scheme for the Five-level NPC VSI fed FPIM drive performance has been presented at steady and transient conditions. The PWM Control is designed in such a way that the post-fault activity of the drive should be continued without any interruption. The controller need not to be changed when fault appears in the drive phases. The five-level torque band is used to reduce the torque ripple in post-fault activity. The proposed Control scheme has verified in Matlab/Simulink results. The findings are shown that the proposed scheme has good post-fault controller for reliability in its operation under the OPF condition.

## REFERENCES

- [1] Y. Song and B. Wang, "Survey on reliability of power electronic systems," *IEEE Trans. Power Electron.*, vol. 28, no. 1, pp. 591–604, Jan 2013.
- [2] B. Chikondra, U. R. Muduli, and R. K. Behera, "Performance comparison of five-phase three-level NPC to five-phase two-level VSI," *IEEE Trans. Ind. Appl.*, vol. 56, no. 4, pp. 3767–3775, 2020.
- [3] E. Levi, "Multiphase electric machines for variable-speed applications," *IEEE Trans. Ind. Electron.*, vol. 55, no. 5, pp. 1893–1909, May 2008.
- [4] B. Chikondra, U. R. Muduli, and R. K. Behera, "An improved DTC technique for three-level NPC VSI fed five-phase induction motor drive to eliminate common mode voltage," in *2019 National Power Electronics Conference (NPEC)*, 2019, pp. 1–6.
- [5] U. R. Muduli and R. K. Behera, "Constant switching frequency DTC SVPWM with reduced common mode voltage for two level five phase induction motor drives," in *2018 IEEE International Conference on Power Electronics, Drives and Energy Systems (PEDES)*, 2018, pp. 1–6.
- [6] U. R. Muduli, A. R. Beig, K. A. Jaafari, J. Y. Alsawalhi, and R. K. Behera, "Interrupt free operation of dual motor four-wheel drive electric vehicle under inverter failure," *IEEE Trans. Transp.*, pp. 1–1, 2020.
- [7] P. Kumar, D. V. Bhaskar, U. R. Muduli, A. R. Beig, and R. K. Behera, "Iron loss modelling with sensorless predictive control of pmbldc motor

drive for electric vehicle application,” IEEE Transactions on Transportation Electrification, pp. 1–1, 2020.

[8] U. R. Muduli, A. R. Beig, K. Al Jaafari, J. Y. Alsawalhi, and R. K. Behera, “An improved direct torque control with battery power management of open-end winding induction motor drive for electric vehicles,”

[9] S. B. Veeranna, U. R. Yaragatti, and A. R. Beig, “Synchronized svpwm algorithm for overmodulation region for three-level vsi,” in IECON 201 - 36th Annual Conference on IEEE Industrial Electronics Society, 2010, pp. 1004–1010.

[10] A. Dekka, A. R. Beig, S. Kanukollu, and M. S. Al Rahis, “Retrofitting of harmonic power filters in onshore oil drilling rigs: Challenges and solutions,” IEEE Transactions on Industry Applications, vol. 50, no. 1, pp. 142–154, 2014.

[11] G. S. Buja and M. P. Kazmierkowski, “Direct torque control of PWM inverter-fed AC motors - a survey,” IEEE Trans. Ind. Electron., vol. 51, no. 4, pp. 744–757, 2004.

[12] S. Payami, R. K. Behera, and A. Iqbal, “DTC of three-level NPC inverter fed five-phase induction motor drive with novel neutral point voltage balancing scheme,” IEEE Trans. Power Electron., vol. 33, no. 2, pp. 1487–1500, Feb 2018.

[13]. Nitta N, W I. Nitta N, Wu F, Lee JT, Yushin G Li-ion battery materials: present and future. Mater Today 18(5):252–264

[14]. Earl T, Mathieu L, Cornelis S, Kenny S, Ambel CC, Nix J (2018) Analysis of long haul battery electric trucks in EU. In: 8th Commercial vehicle workshop, Graz (2018)

[15]. International Energy Agency (2019) Global EV outlook 2019. International Energy Agency



**Jampana Vijay kumar raju**, is pursuing Master degree in Power Electronics and Electric Drives in Avanthi’s st Theresa institute of engineering and technology affiliated to JNTUK Kakinada.



**Mr. B. venkataramana** is currently the Assot Professor and Head of EEE Department. He had worked in different capacities in technical institutions of higher learning for a period of over fifteen years.. He has over 25 publications in International and National Journals/Conferences.